Unclassified
Security Classification

AD-743 959

DOCUMENT CONTROL DATA - R&D

(Security classification of title, body of abstract and indexing annotation must be entered when the overall report is classified)

1. ORIGINATING ACTIVITY *(Corporate author)*
Air Force Cambridge Research Laboratories (LKC)
L.G. Hanscom Field
Bedford, Massachusetts 01730

2a. REPORT SECURITY CLASSIFICATION
Unclassified

2b. GROUP

3. REPORT TITLE
SCATTERING OF HF RADIO WAVES BY A SPHERICAL ELECTRON CLOUD

4. DESCRIPTIVE NOTES *(Type of report and inclusive dates)*
Scientific. Interim.

5. AUTHOR(S) *(First name, middle initial, last name)*
Milton M. Klein

6. REPORT DATE	7a. TOTAL NO. OF PAGES	7b. NO. OF REFS
11 April 1972	11	5

8a. CONTRACT OR GRANT NO.	9a. ORIGINATOR'S REPORT NUMBER(S)
b. PROJECT, TASK, WORK UNIT NOS. 7635-13-01	AFCRL-72-0238
c. DOD ELEMENT 62101F	9b. OTHER REPORT NO(S) *(Any other numbers that may be assigned this report)*
d. DOD SUBELEMENT 681300	

10. DISTRIBUTION STATEMENT
Approved for public release; distribution unlimited.

11. SUPPLEMENTARY NOTES	12. SPONSORING MILITARY ACTIVITY
Reprinted from Radio Science, Vol. 7, No. 2, pp. 257-267, February 1972.	Air Force Cambridge Research Laboratories (LKC) L.G. Hanscom Field Bedford, Massachusetts 01730

13. ABSTRACT

Numerical and analytic solutions in the ray-optics region have been obtained for the scattering of HF radio waves by a spherical electron cloud with a Gaussian distribution of electron density in the radial direction. The results show that a highly overdense or hard cloud has a wide range of backscatter angles for which the cross section is almost constant with a value close to that of an equivalent conducting sphere (critical radius size). A slightly overdense or soft sphere has a much narrower range of almost constant cross section whose value is proportional to the fourth power of the critical radius and considerably below that of an equivalent conducting sphere. In the region of forward scatter, all spheres have essentially the same cross section, independent of hardness. For underdense spheres, the cross section is generally the same as that characteristic of forward scattering except in the region of maximum deflection where the cross section increases very sharply. It is found that when an underdense sphere becomes critical, the maximum deflection is 90°, whereas an overdense sphere retains its maximum deflection of 180° at the critical density. For overdense spheres, the analytic results are in good agreement with those obtained numerically; but for underdense spheres, they are not in good agreement at the higher electron densities.

12

KEYWORDS: Scattering, Radio frequency, Plasma cloud, Ray optics

DD FORM 1 NOV 65 1473

Radio Science, Volume 7, Number 2, pages 257-267, February 1972

Scattering of HF radio waves by a spherical electron cloud

Milton M. Klein

Air Force Cambridge Research Laboratories
L. G. Hanscom Field, Bedford, Massachusetts 01730

(Received March 18, 1971; revised August 16, 1971.)

Numerical and analytic solutions in the ray-optics region have been obtained for the scattering of HF radio waves by a spherical electron cloud with a Gaussian distribution of electron density in the radial direction. The results show that a highly overdense or hard cloud has a wide range of backscatter angles for which the cross section is almost constant with a value close to that of an equivalent conducting sphere (critical radius size). A slightly overdense or soft sphere has a much narrower range of almost constant cross section whose value is proportional to the fourth power of the critical radius and considerably below that of an equivalent conducting sphere. In the region of forward scatter, all spheres have essentially the same cross section, independent of hardness. For underdense spheres, the cross section is generally the same as that characteristic of forward scattering except in the region of maximum deflection where the cross section increases very sharply. It is found that when an underdense sphere becomes critical, the maximum deflection is 90°, whereas an overdense sphere retains its maximum deflection of 180° at the critical density. For overdense spheres, the analytic results are in good agreement with those obtained numerically; but for underdense spheres, they are not in good agreement at the higher electron densities.

1. INTRODUCTION

In recent years, studies of the upper atmosphere have been conducted with artificial ionized clouds obtained by the release of barium vapor at high altitudes. To help in the understanding and interpretation of experimental data, a theoretical study is being made of the scattering of radio waves by an artificial electron cloud.

Because the electron cloud, which is several kilometers in extent, is considerably larger than a typical wavelength in the HF band, the method of geometrical optics has been utilized. For those frequencies at which the effect of the magnetic field is not negligible, a detailed ray-tracing technique such as that furnished by the Haselgrove method [*Haselgrove*, 1955] must be employed. If, however, the magnetic field can be neglected, the scattering may be computed directly, at least for the case of spherical symmetry, with increased accuracy and considerable reduction in computational labor.

Our present investigation is concerned with the frequencies at which the magnetic field is negligible. We shall assume that the distribution of electron density is spherically symmetric and, as indicated by diffusion theory, has a Gaussian form in the radial direction. The collision frequency within the cloud is generally small compared to the incident frequency; thus absorption may be neglected in our calculations.

2. ANALYSIS

A ray initially a distance b from the z axis is deflected through an angle β at a given position r, ϕ within the cloud, and is scattered through an angle θ as it emerges from the cloud (Figure 1). For a spherically symmetric plasma, the scattering is independent of meridian angle and can be described in terms of the scattering angle θ in the plane of incidence and the impact parameter b. The relation between b and θ may be obtained from the scattering integral for the two-body central force problem [*Goldstein*, 1950*a*] and the analogy between particle dynamics and ray optics [*Goldstein*, 1950*b*], or by direct consideration of the scattering of a ray by a spherically symmetric plasma [*Kelso*, 1964]. We may express this relation in the form

$$\frac{\pi - \theta}{2} = b \int_{r_1}^{\infty} \frac{dr}{(\mu^2 r^4 - b^2 r^2)^{1/2}} \qquad (1)$$

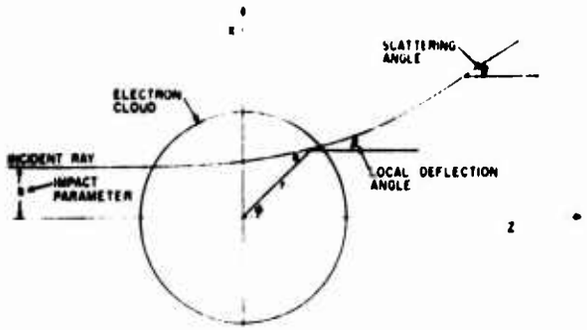

Fig. 1. Sketch showing ray path and scattering parameters.

where μ is the index of refraction, r the radial position of the ray, and r_t the turning point or reflection point, that is, the location at which the ray starts to move away from the center of the sphere. For a Gaussian distribution, the electron density N and the index of refraction have the form

$$N/N_{max} = \exp(-r^2/a^2) \tag{2}$$

and

$$\mu^2 = 1 - N/N_{cr} = 1 - \exp[(r_{cr}^2 - r^2)/a^2] \tag{3}$$

where a is the Gaussian radius and the subscripts max and cr refer to maximum and critical values, respectively. It is convenient to change the variable of integration to $x = a/r$ and to take a as the unit of length to yield

$$\frac{\pi - \theta}{2} = b\int_0^{x_t} \frac{dx}{(\mu^2 - b^2x^2)^{1/2}} \tag{4}$$

and

$$\mu^2 = 1 - \exp(x_{cr}^2 - x^{-2}) \tag{5}$$

The differential cross section in the direction θ, $\sigma(\theta)$, is then calculated by

$$\sigma(\theta) = (4\pi b/\sin\theta)(db/d\theta) \tag{6}$$

Equations 4 and 6 can always be solved numerically for a given variation of μ^2 with x. An approximate analytic solution may be obtained, however, if the function μ^2 may be fitted with reasonable accuracy by a linear or quadratic function of x, since the integral in (4) can then be expressed in terms of elementary functions. The properties of the cross section and its dependence upon the governing parameters in a given region of interest can then be clearly exhibited. For a highly overdense plasma (large r_{cr}), the turning point occurs at a large value of r so that μ^2 varies very rapidly over a small range of x well inside the inflection point which occurs at $x = (2/3)^{1/2}$. We do not expect, therefore, the details of the variation to be very important and should obtain a reasonably accurate solution. However, for a slightly overdense plasma (small r_{cr}) at small impact parameters, the turning point occurs at a small value of r with a consequent slow variation of μ^2 over a wide range of x which includes the inflection point. The manner of variation is important here, and we anticipate more difficulty and less accuracy in obtaining approximate solutions. Since a ray penetrates very little into a highly overdense plasma and deeply into a slightly overdense plasma, it is convenient to refer to these cases as 'hard' and 'soft' spheres, respectively. When the plasma becomes underdense, the turning point is, as in the slightly overdense case, small at small impact parameters; and, in addition, the scattering is now confined to the forward region ($\theta \leqq 90°$). We may therefore consider the underdense case as a 'very soft' sphere and expect difficulties in obtaining an approximate solution.

3. ANALYTIC PROCEDURE

In view of the somewhat different treatments required, the overdense (hard, intermediate, and soft) and the underdense spheres are treated separately.

3.1. Hard sphere. We consider first a typical hard sphere with $r_{cr} = 2$, for which a plot of μ^2 against x is given in Figure 2. Because of the rapid drop in μ^2, it is more accurate to use a single quadratic term than a combination of linear and quadratic terms and write

$$\begin{aligned} \mu^2 &= 1 && x \leqq x_2 \\ \mu^2 &= 1 - a_2(x - x_2)^2 && x \geqq x_2 \end{aligned} \tag{7}$$

where x_2 is the point at which the parabola starts and is determined by noting where μ^2 for the Gaussian has not yet decreased significantly from unity. The constant a_2 may be evaluated by noting that $\mu = 0$ at $x_{cr} = 0.5$ to give $a_2 = 44.5$. A plot of μ^2 for the parabola shows that it is in good agreement with the exact curve over the entire range.

The scattering integral can then be written as

$$\frac{\pi - \theta}{2} = b\int_0^{x_2} \frac{dx}{(1 - b^2x^2)^{1/2}} + b\int_0^{x_1} \frac{du}{(A - Bu - Cu^2)^{1/2}} \tag{8}$$

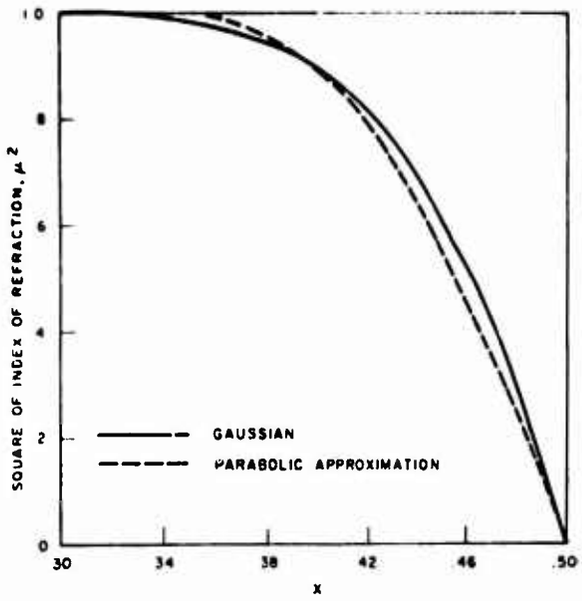

Fig. 2. Plot of μ^2 for hard sphere ($r_{cr} = 2$) and approximation by parabola.

where $A = 1 - b^2x_2^2$, $B = 2b^2x_2$, $C = a_2 + b^2$, and $u = x - x_2$ is the variable of integration.

Performing the integration and noting that the quadratic vanishes at the turning point, we obtain

$$\frac{\pi - \theta}{2} = \sin^{-1} bx_2 + \frac{b}{(a_2 + b^2)^{1/2}} \cdot \left(\frac{\pi}{2} - \sin^{-1} \frac{b^2x_2}{[b^2 + a_2(1 - b^2x_2^2)]^{1/2}}\right) \quad (9)$$

For a hard sphere, a_2 is large compared to b^2 over most of the scattering range, except near forward scattering where b achieves its maximum value of $1/x_2$. We may then neglect the second arc sine term in (9) and write

$$\frac{\pi - \theta}{2} = \sin^{-1} bx_2 + \frac{\pi}{2} \frac{b}{a_2^{1/2}} \quad (10)$$

Solving for b and taking $b/a_2^{1/2}$ as small compared to unity, we obtain

$$b = \frac{\cos(\theta/2)}{x_2[1 + (\pi/2)(a_2x_2^2)^{1/2} \sin(\theta/2)]} \quad (11)$$

which yields the cross section

$$\sigma(\theta) = \frac{\pi}{x_2^2} \frac{1 + (\pi/2)\csc(\theta/2)(a_2x_2^2)^{1/2}}{[1 + (\pi/2)\sin(\theta/2)(a_2x_2^2)^{1/2}]^4} \quad (12)$$

An analysis of (9) and (11) shows that the cross-section formula given by (12) is valid for hard spheres from the backscatter region to about 30° in the forward-scatter region. Therefore, to complete our calculation, we require the cross section for small scattering angles in the forward direction.

Because we are interested in small values of θ and hence values of x where the electron density is small, we approximate μ^2 by the linear function

$$\mu^2 = 1 - a_0(x - x_0) \quad (13)$$

where x_0 is a cutoff position at which the electron density is negligibly small. The coefficient a_0 is determined from the slope of the μ^2 versus x curve at x_0; that is,

$$a_0 = -(2/x_0^3) \exp(x_{cr}^2 - x_0^{-2}) \quad (14)$$

The scattering integral is then

$$\frac{\pi - \theta}{2} = \sin^{-1} bx_0 + b \int_{x_t}^{x_{cr}} \frac{dx}{[1 - a_0(x - x_0) - b^2x^2]^{1/2}} \quad (15)$$

For large impact parameter, x_t is close to x_0; we may therefore approximate $1 - b^2x^2$ by $2(1 - bx)$ to give

$$\frac{\pi - \theta}{2} = \sin^{-1} bx_0 + b \int_{x_t}^{x_{cr}} \frac{dx}{[(2 + a_0x_0) - (2b + a_0)x]^{1/2}} = \sin^{-1} bx_0 + [2b/(2b + a_0)][2(1 - bx_0)]^{1/2}$$

The term bx_0 is close to unity; therefore, we can write

$$\sin^{-1} bx_0 \cong \frac{\pi}{2} - [2(1 - bx_0)]^{1/2}$$
$$\frac{\theta}{2} = \left(1 + \frac{2}{a_0x_0}\right)^{-1} [2(1 - bx_0)]^{1/2} \quad (16)$$

which yields the cross section

$$\sigma(\theta) = \frac{\pi}{x_0^2}\left(1 + \frac{2}{a_0x_0}\right)^2 - \frac{\pi}{x_0^2}\frac{\theta^2}{8}\left(1 + \frac{2}{a_0x_0}\right)^4 \quad (17)$$

It is interesting to note that no change is produced in (16) if we use in addition to the linear term in (13) a quadratic term $b_0(x - x_0)^2$. This result is not unexpected; the integrand is linear in the small quantity $1 - bx$ and, therefore, terms of higher order than the first in the small quantity $(x - x_0)$ are negligible.

Because the cross section becomes infinite for zero-scattering angle, it is convenient to adopt a cut-off value for the impact parameter so that a large but

finite cross section is obtained. A reasonable requirement is to take the electron density N_0/N_{cr} at x_0 between 10^{-2} and 10^{-3}. Using (5) and (14) we express the cross section at $\theta = 0$ by

$$\sigma(\theta) = \frac{\pi}{x_0^2}\left(1 + \frac{x_0^2}{N_0/N_{cr}}\right) \tag{18}$$

where x_0 is determined by

$$x_0^{-2} = x_{cr}^{-2} + \log(N_{cr}/N_0) \tag{19}$$

3.2. Intermediate case. If the sphere is moderately hard, the critical value x_{cr} will be somewhat greater than the point of inflection which will affect the right side of the curve. We take as typical examples $r_{cr} = 1$ and $r_{cr} = 1/2$ for which plots of μ^2 against x are shown in Figures 3 and 4. For the case $r_{cr} = 1$ (Figure 3) we see that, aside from the bending in the region $\mu \cong 1$, the curve is almost a straight line over the remaining region. Although it is possible to use a parabola over the initial portion of the curve and a straight line over the remainder, the resulting formulas become sufficiently complicated to make analysis and numerical calculation difficult. We shall, therefore, use a straight line starting at $x = 0.54$, $\mu = 1$ to $x_{cr} = 1.0$, $\mu_{cr} = 0$. The initial portion of the curve from $x = 0.54$ to $x = 0.6$, while not accurate should not affect the remainder very much since it is a small part of the integral in (4) over most of the range. Furthermore, because it is above the exact curve in the initial region, this should compensate somewhat for the straight line being, on the

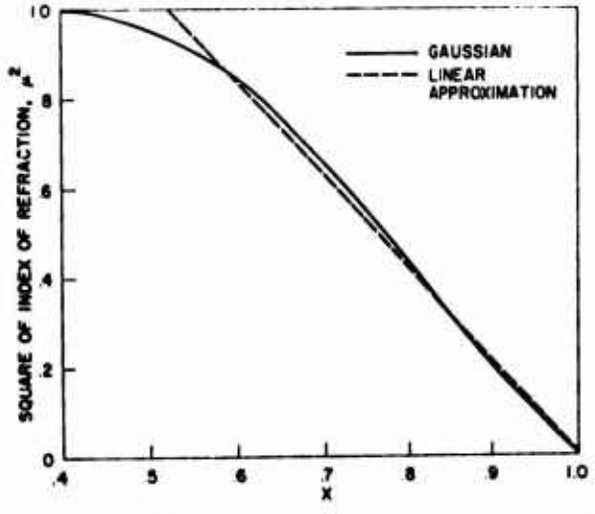

Fig. 3. Plot of μ^2 for moderately hard sphere ($r_{cr} = 1$) and approximation by single straight line.

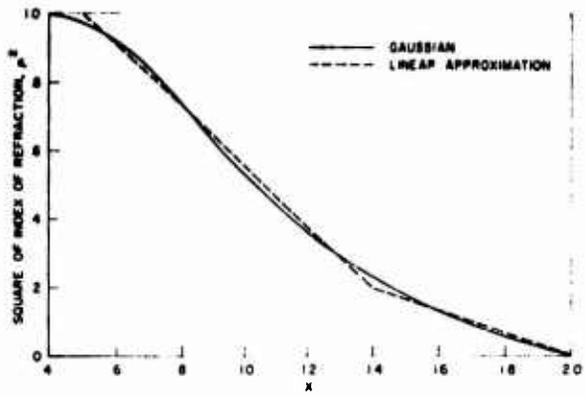

Fig. 4. Plot of μ^2 for moderately soft sphere ($r_{cr} = \frac{1}{2}$) and approximation by two straight lines.

average, slightly below the exact curve in the remaining region. Our straight line can be written as

$$\begin{aligned} \mu^2 &= 1 && x \leqq x_1 \\ \mu^2 &= 1 - a_1(x - x_1) && x \geqq x_1 \end{aligned} \tag{20}$$

for which the scattering integral yields

$$\frac{\pi - \theta}{2} = \sin^{-1} bx_1 + \frac{\pi}{2} - \sin^{-1}\frac{a_1 + 2b^2x_1}{[a_1^2 + 4b^2(1 + a_1x_1)]^{1/2}} \tag{21}$$

The arc sine terms may be combined in a simple manner and the parameter b solved for explicitly as a function of scattering angle. We obtain

$$b = x_1^{-2}\cos(\theta/2)\cdot\left[1 + \frac{4}{a_1x_1}\left(1 + \frac{1}{a_1x_1}\right)\sin^2\frac{\theta}{2}\right]^{-1/2} \tag{22}$$

which yields the cross section

$$\sigma(\theta) = \frac{\pi}{x_1^2}\left[\frac{1 + 2/a_1x_1}{1 + 4/a_1x_1(1 + 1/a_1x_1)\sin^2(\theta/2)}\right]^2 \tag{23}$$

An analysis of (19) shows that when the turning point = 0.6, the corresponding angle is less than 30°; thus the cross-section formula can be used to at least 30°. The cross section near zero scattering can then be obtained from (17).

As the critical radius decreases to 0.5, Figure 4 shows that the right-hand portion of the $\mu^2 - x$ curve becomes concave upward so that the curve may no longer be fitted accurately by a single straight line. It is possible, however, to obtain good accuracy by the

use of two straight lines of different slopes meeting at $x = 1.4$. The cross section corresponding to turning points within the region of the first straight line may be obtained from (23). When the turning point lies beyond the region of the first straight line, the contribution to the scattering integral from the second line must be considered. Because of the discontinuity in the slope, the integral loses its simple structure and can no longer be solved in simple analytic form for arbitrary b. However, for small b (large scattering angles), the integral assumes a simple form and can be conveniently solved. For turning points beyond x_2 the scattering integral is

$$\frac{\pi - \theta}{2} = \sin^{-1} bx_1 + \sin^{-1} \frac{a_1 + 2b^2 x_2}{[a_1^2 + 4b^2(1 + a_1 x_1)]^{1/2}} - \sin^{-1} \frac{a_1 + 2b^2 x_1}{[a_1^2 + 4b^2(1 + a_1 x_1)]^{1/2}} + \frac{\pi}{2} - \sin^{-1} \frac{a_2 + 2b^2 x_2}{[a_2^2 + 4b^2(\mu_2^2 + a_2 x_2)]^{1/2}} \quad (24)$$

For small b, the arguments of the arc sine terms may be expanded to first order in b^2 to yield

$$\frac{\pi - \theta}{2} = \sin^{-1} bx_1 + \sin^{-1}\left(1 - \frac{2b^2}{a_1^2}\mu_2^2\right) - \sin^{-1}\left(1 - \frac{2b^2}{a_1^2}\right) + \frac{\pi}{2} - \sin^{-1}\left(1 - \frac{2b^2}{a_2^2}\mu_2^2\right) \quad (25)$$

where we have used

$$\mu_2^2 = 1 - a_1(x_2 - x_1)$$

Expanding the arc sine terms for small b, we obtain

$$\frac{\pi - \theta}{2} = b\left[x_1 + \frac{2}{a_1 x_1}(1 - \mu_2) + \frac{2\mu_2}{a_2}\right] \quad (26)$$

which yields the cross section

$$\sigma(\theta) = \frac{\pi}{x_1^2} \frac{(\pi - \theta)}{\sin \theta} \left[1 + \frac{2}{a_1 x_1}(1 - \mu_2) + \frac{2\mu_2}{a_2 x_1}\right] \quad (27)$$

valid for large scattering angles.

3.3. Soft sphere. When the critical radius is small, the initial moderate decrease in μ^2 is followed by a very slow decrease, as shown in Figure 5 for $r_{cr} = 1/8$. It becomes difficult and inaccurate, therefore, to use a combination of two simple curves. However, we have found it feasible to use a straight line for the initial portion of the curve, and an approximate method of integration for the latter portion.

A reasonable fit up to $x = 1.4$ may be obtained with a straight line from $x_1 = 0.5$, $\mu^2 = 1.0$, to $x_2 = 1.4$. The cross section may then be obtained from (22) and (23) as long as the parameter b does not go below the value corresponding to x_2 as the turning point, that is, $b = \mu_2/x_2$. The calculation then yields a maximum scattering angle of about 69°.

For values of x beyond x_2 we split the integral at a suitable point x_3 where x_3 is not far from x_2, but

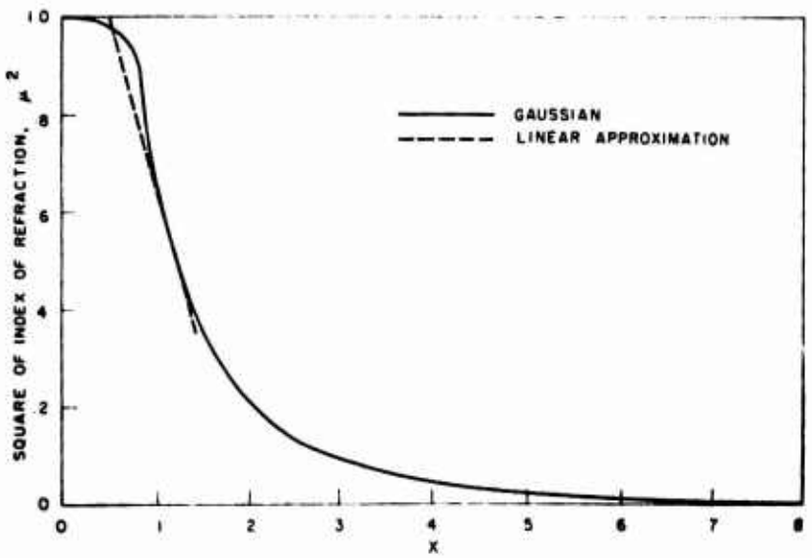

Fig. 5. Plot of μ^2 for very soft sphere ($r_{cr} = 1/8$) and approximation by straight line for initial position of curve.

such that x_3^2 is somewhat larger than unity and write

$$I = I_1 + I_2 \tag{28a}$$

where

$$I_1 = \int_{x_1}^{x_3} \frac{b\,dx}{(\mu^2 - b^2x^2)^{1/2}} \tag{28b}$$

$$I_2 = \int_{x_3}^{x_2} \frac{b\,dx}{(\mu^2 - b^2x^2)^{1/2}} \tag{28c}$$

The integral I_1 may be evaluated approximately by noting that μ has not changed very much in the interval and, therefore, may be taken as constant. We obtain

$$I_1 = \sin^{-1}\frac{bx_3}{\langle\mu\rangle} - \sin^{-1}\frac{bx_2}{\langle\mu\rangle} \tag{29}$$

where $\langle\mu\rangle$ is an average value in the interval. To integrate I_2, we assume x_3^2 is sufficiently greater than unity so that a series expansion of μ^2 may be used. We then have

$$\mu^2 = 1 - \exp(x_{cr}^{-2} - x^{-2}) \tag{30a}$$

$$\cong x^{-2} - x_{cr}^{-2} \tag{30b}$$

The integral I_2 now takes the form

$$I_2 = \int_{x_3}^{x_1} \frac{bx_{cr}x\,dx}{(x_{cr}^2 - x^2 - b^2x_{cr}^2x^4)^{1/2}} \tag{31}$$

and may be integrated to yield

$$I_2 = \frac{\pi}{4} - \frac{1}{2}\sin^{-1}\frac{1 + 2b^2x_{cr}^2x_3}{(1 + 4x_{cr}^4b^2)^{1/2}} \tag{32}$$

For values of θ greater than and near $\pi/2$, the b^2 term in the numerator is comparable to unity whereas the b^2 term in the denominator is much greater than unity. It is not until θ is in the range near π that the latter term becomes comparable to unity. We find it convenient, therefore, to calculate near $\pi/2$ and near π. For θ near $\pi/2$, the arc sine terms in I_1 and I_2 are small compared to unity, and we may write our scattering integral as

$$\pi/2 - \theta = (A - x_3^2)\,b - (2x_{cr}^2b)^{-1} \tag{33}$$

where $A = 2[x_1 + (x_3 - x_2)/\langle\mu\rangle]$. Solving for b, we obtain

$$b = \frac{1}{2(A - x_3^2)}\left\{\frac{\pi}{2} - \theta + \left[\left(\frac{\pi}{2} - \theta\right)^2 + 4\frac{(A - x_3^2)}{2x_{cr}^2}\right]^{1/2}\right\} \tag{34}$$

which yields the cross section

$$\sigma(\theta) = \frac{\pi}{\sin\theta}\frac{1}{x_{cr}^4(A - x_3^2)^2} \cdot\left\{\left(\frac{\pi}{2} - \theta\right) + \left[\left(\frac{\pi}{2} - \theta\right)^2 + 2\frac{A - x_3^2}{x_{cr}^2}\right]^{1/2}\right\} \cdot\left[\left(\frac{\pi}{2} - \theta\right)^2 + 2\frac{A - x_3^2}{x_{cr}^2}\right]^{-1/2} \tag{35}$$

In terms of b, the cross section has the simpler form

$$\sigma(\theta) = \frac{8\pi}{\sin\theta}\frac{x_{cr}^2b^3}{1 + 2(A - x_3^2)x_{cr}^2b^2} \tag{36}$$

For large scattering angles, the argument of the arc sine term in the I_2 integral is no longer small compared to unity; thus the preceding simplification cannot be used. We therefore write the scattering integral in the form

$$\pi - \theta = Ab + \cos^{-1}\frac{1 + 2b^2x_{cr}^2x_3^2}{(1 + 4x_{cr}^4b^2)^{1/2}} \tag{37}$$

and take the cosine of both sides to yield

$$\cos(\pi - \theta) = \cos(Ab)\frac{1 + 2x_{cr}^2x_3^2b^2}{(1 + 4x_{cr}^4b^2)^{1/2}} - 2b\sin(Ab)x_{cr}^2\left(\frac{1 - x_3^2/x_{cr}^2}{1 + 4x_{cr}^4b^2}\right)^{1/2}$$

Since Ab is a small quantity, we may expand cos (Ab) and b sin (Ab) to first order in b^2 and solve for b to obtain

$$b = \sin(\pi - \theta)/2x_{cr}^2[B + \cos^2(\pi - \theta)]^{1/2} \tag{38}$$

where

$$B = \frac{A}{x_{cr}^2}\left(1 - \frac{x_3^2}{x_{cr}^2}\right)^{1/2} - \frac{x_3^2}{x_{cr}^2} + \frac{A^2}{4x_{cr}^4}$$

The cross section is, accordingly,

$$\sigma(\theta) = \frac{\pi}{x_{cr}^4}\frac{(1 + B)\cos(\pi - \theta)}{[B + \cos^2(\pi - \theta)]^2} \tag{39}$$

For backscatter, we obtain the interesting limiting form (neglecting the small quantity B)

$$\sigma(\theta) = \pi/x_{cr}^4 \tag{40a}$$

$$r_{eff} = r_{cr}^2 \tag{40b}$$

where r_{eff} is the radius of a conducting sphere having the same cross section as the Gaussian sphere.

3.4. Underdense sphere. When the maximum electron density of the plasma is below the critical frequency, the index of refraction has a minimum

value greater than zero. The general shape of the curve is similar to a soft sphere, with the minimum value approached asymptotically for large x. In view of the tediousness of our method for very soft spheres, we use a perturbation technique in which we assume in first approximation that the deflection of the ray path may be neglected. For a spherical plasma, the relation between index of refraction and the angle α between the radius and the ray direction is given by Bouger's rule [*Kelso*, 1964]

$$\mu r \sin \alpha = b \tag{41}$$

The variation in α due to change in μ is

$$d\alpha = -\frac{\tan \theta}{2\mu^2} \frac{d(\mu^2)}{dr} dr \tag{42}$$

where we omit the change in α due to the explicit r term since this gives its variation due to the angular change in r (note that for fixed μ and hence no deflection, the variation in r gives precisely the change in α). Since $d\alpha$ is referred to a fixed position of r, it gives the deflection of the ray at this point. The total deflection of the ray is then obtained by integration over the ray path. If we assume the path is unperturbed then $\tan \alpha = b/z$, $r^2 = b^2 + z^2$, and the integral can be cast in the form

$$\theta = \frac{b}{2} \int_{-\infty}^{\infty} \frac{1}{\mu^2} \frac{d(\mu^2)}{dr} \frac{dz}{r} \tag{43}$$

a relation similar to that obtained in classical mechanics [*Bohm*, 1951] if we take μ^2 as close to unity. For our Gaussian sphere $\mu^2 = 1 - \rho e^{-r^2}$ where $\rho = N_{max}/N_{cr}$, yielding

$$\theta = \rho b^2 e^{-b^2} \int_{\infty}^{\infty} \frac{e^{-b^2u^2}}{1 - \rho e^{-b^2} e^{-b^2u^2}} du \tag{44}$$

where $u = z/b$. Since ρ is less than unity, we may expand the denominator to effect the integration and obtain

$$\theta = \pi^{1/2} c b \left(1 + \frac{c}{2^{1/2}} + \frac{c^2}{3^{1/2}} + \cdots\right) \tag{45}$$

where $c = \rho e^{-b^2}$, which yields the cross section

$$\sigma(\theta) = \frac{4\pi^{1/2} b}{\sin \theta} \left\{c\left[(1 - 2b^2) + (1 - 4b^2) \frac{c}{2^{1/2}} + (1 - 6b^2) \frac{c^2}{3^{1/2}} + \cdots\right]\right\}^{-1} \tag{46}$$

For underdense spheres, the scattering angle vanishes at $b = 0$ as well as at large b so that b is a double valued function of θ; accordingly, the contributions from the two values of b must be added numerically to obtain the total cross section. The scattering in the forward direction may be calculated by the procedure for overdense spheres. However, since ρ is less than unity, we express (19) directly in terms of

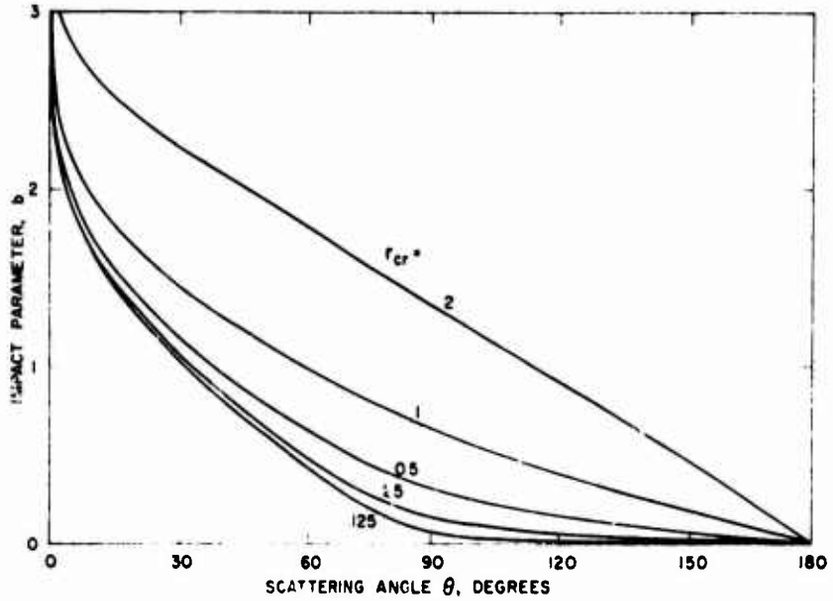

Fig. 6. Variation of impact parameter with scattering angle for overdense spheres for several values of critical radius.

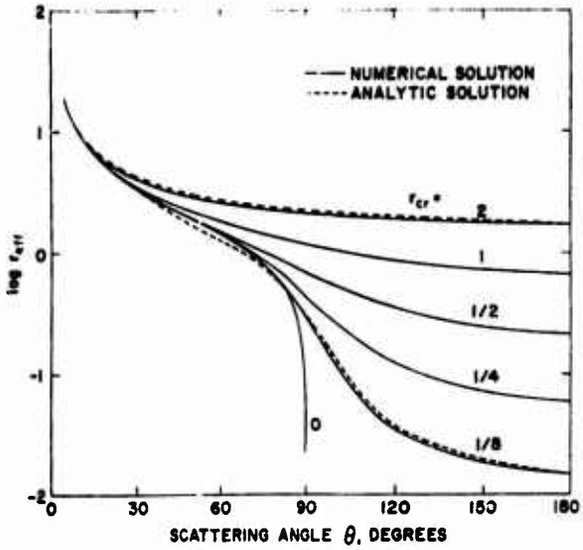

Fig. 7. Variation of effective radius with scattering angle for several values of critical radius.

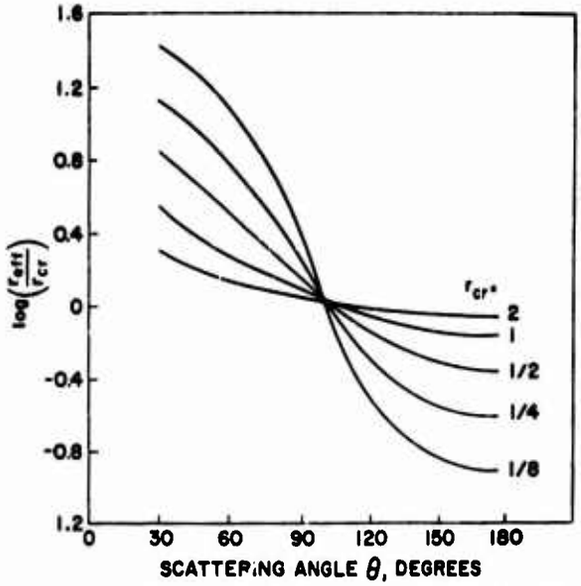

Fig. 8. Plot of ratio of effective radius to critical radius against scattering angle for overdense spheres with critical radius as the parameter.

ρ by

$$x_0^{-2} = \ln (N_{cr}/N_0) - \ln \rho^{-1} \qquad (47)$$

4. RESULTS AND DISCUSSION

The results obtained by the numerical procedure for overdense spheres are presented in Figures 6 and 7, where we have plotted the variation of impact parameter and cross section with scattering angle, with the cross section expressed in terms of r_{eff}. The results obtained by the analytic procedure were generally very close to those obtained numerically. To indicate the agreement obtained, we have also plotted in Figure 7 the analytic solutions for r_{eff} for a hard

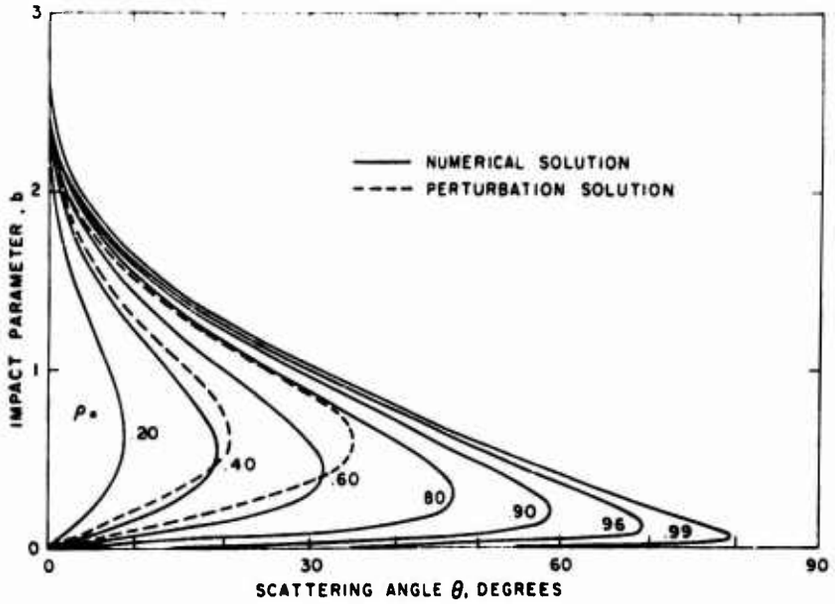

Fig. 9. Variation of impact parameter with scattering angle for underdense spheres for several values of density ratio.

sphere ($r_{cr} = 2$) and for a very soft sphere ($r_{cr} = 1/8$).

Figure 6 indicates that for hard spheres, except for the forward-scattering region, the impact parameter is almost a linear function of scattering angle. As the critical radius becomes small, the impact parameter decreases rapidly in the forward-scattering region, resulting in very small values for all scattering angles greater than 90°.

Figure 7 shows that hard spheres have an almost constant cross section over a fairly wide range of backscattering angles, and r_{eff} is only slightly less than r_{cr}. For $r_{cr} = 0$, the cross section becomes vanishingly small from 0 = 90° to 180°. We have indicated this result by a vertical line at 90°. The small values of r_{eff} for a soft sphere in the backscatter region are due to the great depth of penetration, and consequently small value of the impact parameter b required for a given scattering angle. The rate of change of impact parameter with scattering angle is accordingly very small in the backscatter region, resulting in low cross sections. We thus have a transition region in which r_{eff} decreases very rapidly until the scattering angle becomes quite large. This result may also be seen from the form of the μ^2 versus x curve for a very soft sphere (Figure 5) and the scattering integral. As the turning point gets closer to the center of the sphere, x_t becomes larger and the integral starts to increase rapidly because of the large contribution from the region of small μ values; the value of b then begins to decrease rapidly with a sharp drop in cross section. For large values of the turning point, however, the integral is quite large and further increases in the scattering angle have very little effect upon $db/d\theta$, resulting in a slowly decreasing cross section.

In the region of forward scatter, we note that the curves for different r_{cr} coalesce, the process occurring at smaller angles for larger r_{cr}. This result occurs because the forward-scattered rays penetrate the outer edge of the cloud where the electron density and its gradient are small, and do not differ significantly for different critical radii. The scattering therefore depends principally upon the impact parameter and very little upon the critical radius. For large values of r_{cr}, however, the electron density is affected to some extent by the critical radius unless the impact parameter is taken sufficiently large. (See equation 19, where we note that large r_{cr} may have some effect unless the cutoff density N_0/N_{cr} is taken sufficiently small.) The curves for large r_{cr}, therefore, coalesce more slowly than do the smaller r_{cr} curves.

Since, in backscatter, the effective radius r_{eff} is very close to r_{cr} for large r_{cr} and decreases as r_{cr}^2 for small r_{cr} (see equation 40), it is of interest to see whether a simple exponential law can be used to represent the backscatter results. A plot of log $(1 - r_{eff}/r_{cr})$ against r_{cr} shows that the backscatter results may be fitted with good accuracy by a straight line whose equation is

$$1 - r_{eff}/r_{cr} = e^{-1.01 r_{cr}} \tag{48}$$

This relation gives the proper dependence of r_{eff} upon r_{cr} for small r_{cr} and satisfies the requirement that r_{eff}/r_{cr} is close to unity for large r_{cr}. To show the relations between r_{eff} and r_{cr} for all scattering angles, we have plotted in Figure 8 the ratio r_{eff}/r_{cr} as a function of scattering angle for several values of r_{cr}.

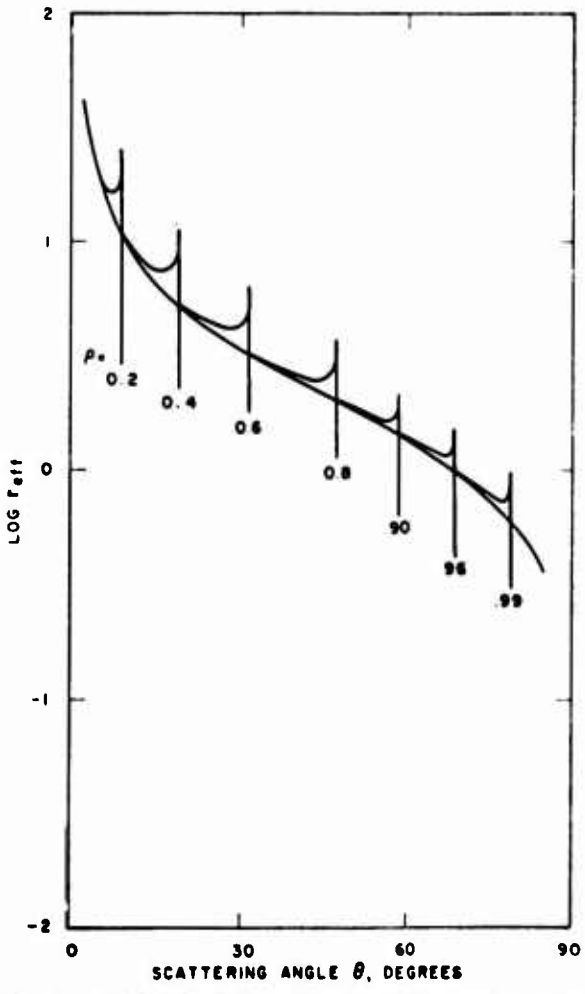

Fig. 10. Variation of effective radius with scattering angle for underdense spheres for several values of density ratio.

The curves cross near $\theta = 105°$ and $r_{eff} \approx r_{cr}$ indicating that, in this scattering region, all Gaussian spheres may be replaced by a conducting sphere of radius equal to the critical radius.

The variation of impact parameter with scattering angle for underdense spheres is shown in Figure 9 where, in contradistinction to the overdense case, small deflections are obtained at small as well as at large values of the impact parameter. The results obtained by the perturbation procedure are in fair agreement with the more exact calculations at small values of the density ratio ρ, the agreement lessening as ρ increases. The more exact calculations show a steady decrease of b at maximum deflection with increasing ρ, whereas the corresponding value of b by the analytic method is relatively insensitive to an increase in ρ. The two sets of curves are therefore considerably displaced at higher values of ρ, with consequently inaccurate cross sections. Attempts to improve the perturbation results by an iterative procedure in which the orbit is not neglected have not proved very successful. We have therefore not presented the analytic results for the cross sections.

The cross-section results are presented in Figure 10, where we have added the contributions from the two values of b. The contribution from the large value of b is generally much higher, except near θ_{max}, where both b values give very large contributions. The vertical lines in Figure 10 indicate the points of maximum deflection at which the cross section is infinite. As anticipated, the curves for different ρ coalesce in the forward-scattering region, with merging occurring at lower values of θ for smaller ρ. This may be easily seen by noting that the value of r_0 depends more strongly on ρ when it is small (see equation 47).

For the purpose of comparison and discussion with respect to the critical density region, some of the impact parameter results for overdense and underdense spheres are presented together in Figure 11. We note that, as the density approaches unity, the upper branch for the underdense region merges with the forward-scatter portion of the overdense curve. In addition, the lower branch of the underdense curve goes to $b = 0$ with a maximum deflection of 90°, while the backscatter portion of the overdense curve also goes to $b = 0$ for the region 90° to 180°.

We thus have a discontinuity in maximum scattering angle at the critical density, with 90° obtained when the approach is from underdense values and 180° when it is from the overdense side.

The cross section approaches zero in the backscatter region as the density becomes critical from the overdense side (see Figure 7) whereas because of the infinite slope in the impact parameter curve, it becomes infinite at 90° from the underdense side (Figure 9).

These peculiarities in the scattering near critical

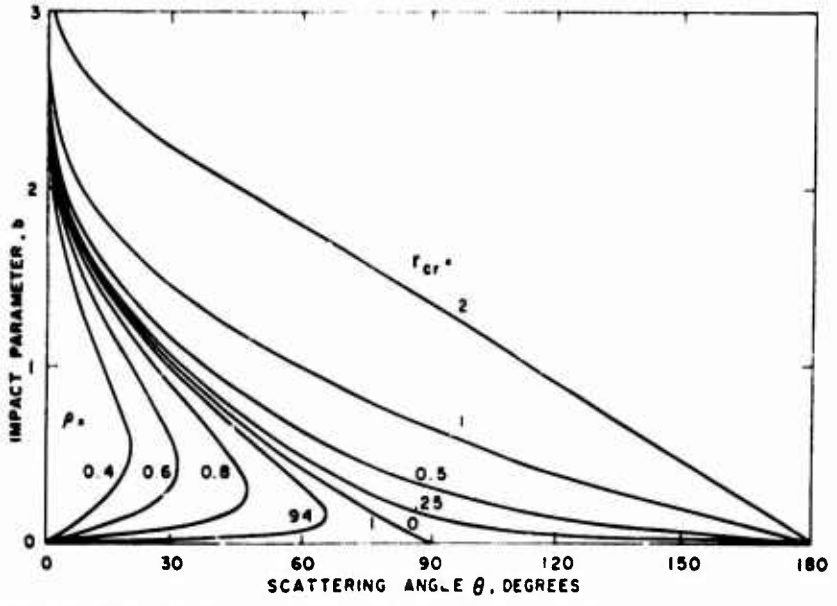

Fig. 11. Plot of impact parameter against scattering angle for underdense and overdense spheres showing limiting forms at critical density.

density are due to the use of a geometric optics model for the calculations. The nature of the scattering in this region may be exhibited in terms of a simple model for the electron density which has the proper asymptotic form near the center of the cloud (large x). We write

$$\mu^2 = 1 - \rho a^2 x^2 \qquad 0 \leqq x \leqq x_1$$
$$\mu^2 = 1 - \rho + \frac{\rho c^2}{x^2} \qquad x \geqq x_1 \tag{49}$$

where a simple parabolic fit has been chosen for small x and an inverse square behavior for large x. The coefficients a and c may be evaluated in terms of a specific density distribution.

The scattering integral now reads

$$\pi - \theta = \frac{2b}{(a^2\rho + b^2)^{1/2}} \sin^{-1} (a^2\rho + b^2)^{1/2} x_1$$
$$+ \frac{\pi}{2} - \sin^{-1} \frac{2b^2 x_1^2 - (1 - \rho)}{[(1 - \rho)^2 + 4\rho c^2 b^2]^{1/2}} \tag{50}$$

For b close to zero the first term is negligible indicating, as expected, that the scattering parameters is determined by the inte center of the sphere. For $b = 0$ we

$$\pi - \theta = (\pi/2) - \sin^{-1} [(1 - \rho)/|$$

which yields $\theta = 0°$ for underdense 180° for the overdense case. At th the limiting value as b approaches addition, the model gives the required of b versus θ near $\theta = 0$ (underdens 180° (overdense).

REFERENCES

Bohm, D. (1951), *Quantum Theory*, c Hall, Inc., New York.

Goldstein, H. (1950*a*), *Classical Mechan* son-Wesley, Reading, Mass.

Goldstein, H. (1950*b*), *Classical Mechan* son-Wesley, Reading, Mass.

Haselgrove, J. (1955), Ray theory and ray tracing, Rep. Conf. Phys. Ionosp Physical Society, London.

Kelso, J. (1964), *Radio Ray Propagation* chap. 5, McGraw-Hill, New York.